Suppression of Co-intercalation on the Carbon Anode by MA Addition in a PC-base Electrolyte

Woo-Seong Kim,[†] Dong-Won Park, Hwan-Jung Jung, and Yong-Kook Choi[*]

[†]*R&D Center, DAEJUNG Chemicals & Metals Co., Ltd., Gyeonggi-do 429-848, Korea*
Department of Chemistry & IBS & RRC/HECS, Chonnam National University, Gwangju 500-757, Korea
[*]*E-mail: ykchoi@chonnam.ac.kr*
Received May 11, 2005

Propylene Carbonate (PC) has the interesting properties of being able to dissolve and dissociate lithium salts, thus leading to highly conducting electrolytes even at low temperatures. Moreover, electrolytes that contain PC are stable against oxidation at voltages up to ~5 V. However, it is known that, when lithium is intercalated into graphite in pure PC based electrolytes, solvent co-intercalation occurs, leading to the destruction of the graphite structure. (*i.e.*, exfoliation). The objective of this study was to suppress PC decomposition and prevent exfoliation of the graphite anode by co-intercalation. Electrochemical characteristics were studied using Kawasaki mesophase fine carbon (KMFC) in different 1 M LiPF$_6$/PC-based electrolytes. Electrochemical experiments were completed using chronopotentiometry, cyclic voltammetry, impedance spectroscopy, X-ray diffraction, and scanning electron microscopy. From the observed results, we conclude that the MA and Li$_2$CO$_3$ additive suppressed co-intercalation of the PC electrolyte into the graphite anode. The use of additives, for reducing the extent of solvent decomposition before exfoliation of the graphite anode, could therefore enhance the stability of a KMFC electrode.

Key Words : Lithium ion battery, Co-intercalation, Propylene carbonate, Methyl acetate, Lithium carbonate

Introduction

Lithium ion batteries are generally composed of a lithium-containing transition metal oxide as the cathode material and graphite as the anode. Graphite represents a promising alternative anode material for replacing lithium metal, for use in rechargeable lithium ion batteries for overcoming safety problems and the short cycle of secondary lithium metal batteries. It has been reported that the charge process involves the intercalation of lithium between the graphene layers. Graphite undergoes a small volume change upon intercalation/de-intercalation and exhibits a high specific capacity, a highly desirable charge potential profile, and superior cycling behavior. However, irreversible reactions that take place with lithium during the first cycle represent one of the very persistent problems associated with the use of graphite as an anode material. On the surface of the graphite electrode, solvents are decomposed during initial intercalation process. Solvent decomposition is not simply co-intercalation. In particular, the graphite structure is destroyed due to solvent co-intercalation when solvent decomposition occurs on a graphite electrode surface.

Propylene carbonate (PC) has some interesting properties, one of which is its ability to dissolve and dissociate lithium salts leading to highly conducting electrolytes, even at low temperatures. Moreover, electrolytes containing PC as a unique solvent are stable against oxidation to voltages ~5 V.[1] However, it is known that when lithium is intercalated into graphite in pure PC based electrolytes, solvent co-intercalation leads to the destruction of the graphite structure. (*i.e.*, exfoliation).[2-9] A number of attempts to suppress PC

decomposition has been reported. Shu *et al.* proposed a method using a crown ether.[10] Aurbach *et al.* reported on the effective influence of carbon dioxide.[5] Najl *et al.* showed the effects of the addition of small amounts of halogenated like Cl-EC, Br-BL or Me-ClF to PC.[11] In the absence of any additives, no reports have appeared on the stable performance of graphitized carbon. In this work, we attempted to suppress solvent decomposition and solvent co-intercalation in PC-base electrolyte by the use of MA and Li$_2$CO$_3$ as additives. Chronopotentiometry, cyclic voltammetry, impedance spectroscopy and conductivity meter were used to investigate the effect of additives (MA, Li$_2$CO$_3$). Scanning electron microscopy (SEM), X-ray diffraction (XRD) were also used to monitor changes in the surface morphology and structure due to the formation of a passivation film caused by solvent decomposition and the precipitation of Li$_2$CO$_3$ which was added to the electrolyte.

Experimental Section

A Kawasaki mesophase fine carbon (KMFC) electrode were prepared by mixing KMFC powder (Kawasaki Co. Ltd.) with polyvinyldifluoride (PVDF) as a binder, followed by pressing onto a copper foil using a stainless steel roller. After vacuum drying at 120 °C for 6 hrs, the electrode was placed in a three-electrode cell. Lithium metal was used as the counter and reference electrodes. The reference electrode was sandwiched between a square KMFC electrode (1 cm^2) and the Li counter electrode was separated with a glassy separator. This procedure was carried out under an atmosphere of argon. The electrochemical properties of solvent

decomposition on the KMFC electrode were investigated using an organic electrolyte system. High-purity propylene carbonate (PC, Aldrich) and Methyl acetate (MA, Aldrich) were used as solvents for the electrolyte solution. Lithium hexafluoro phosphate, $LiPF_6$ (Aldrich) was used as the electrolytic salt. All solvents, electrolytic salts, and the prepared electrolyte were stored in a glove box purged by Ar gas. Lithium carbonate, Li_2CO_3 (Aldrich), was added to the prepared electrolyte. In fact, Li_2CO_3 was found to dissolve with difficulty in the organic solvent and it was necessary to stir the solution for a week to obtain an electrolytic solution. Finally, however, an electrolyte that was saturated with Li_2CO_3 was obtained.

Chronopotentiometry and cyclic voltammetry were used to study the initial irreversible reactions and solvent decomposition. The properties of the passivation film on the KMFC and the first intercalation of Li^+ in KMFC through the passivation film were investigated by a.c. impedance spectroscopy by means of a Potentiostat/Galvanostat (EG&G model 273A) and Lock-in Amplifier (EG&G model 5210). An impedance measurement was performed by applying the previously measured open-circuit potential, overlaid with a 5 mV harmonic perturbation signal in the frequency range from 100 kHz to 10 mHz. These measurements were carried out at room temperature. An SEM analysis of the samples involved the use of a JSM-5400 Scanning Microscope (NORAN Instruments). The working voltage was set at 20 kV and the working distance of the lens was set at 27 md. After charging the KMFC electrode to 0.0 V (*vs.* Li/Li^+) and discharging it to 2.0 V (*vs.* Li/Li^+), the sample was rinsed with MA to remove the electrolyte and dried in a vacuum. XRD measurements (Rigaku D/max-1200) were used to investigate the structure of the Solid Electrolyte Interphase (SEI) film. These measurements were carried out at room temperature.

Results and Discussion

Figure 1 shows the initial charge curve for the KMFC electrode in 1 M $LiPF_6$/pure PC and 1 M $LiPF_6$/PC : DEC (4 : 1, volume ratio) at a low rate of 0.5 mA/cm². The voltage on the initial charge decreased very rapidly from the open circuit voltage (OCV) to 0.9 V (*vs.* Li/Li^+). However, long voltage plateaus were observed at around 0.8 V (*vs.* Li/Li^+), as the result of decomposition of the PC electrolyte, as has been reported previously.[12-18] When lithium in a PC electrolyte is intercalated into the KMFC electrode, solvent co-intercalation and subsequent destruction of the KMFC electrode structure and exfoliation of the graphene layers occurs due to both continuous PC decomposition without stable passivation film formation and continuous PC-Li co-intercalation into the graphene layers. PC decomposition on KMFC electrode is also accompanied by large amounts of gas evolution, which was assumed to be propylene gas. Exfoliation may be enhanced in cases where the reduction of the solvated molecules leads to the production of gas. As the result, in the PC electrolyte, the KMFC electrode did not
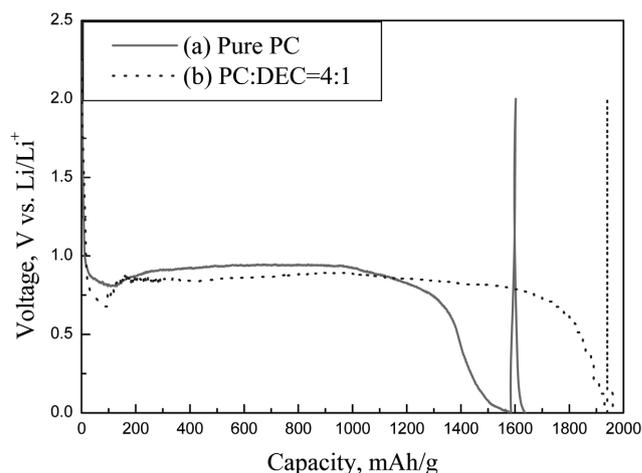

Figure 1. Voltage-capacity profiles of the KMFC electrode in (a) 1 M $LiPF_6$/pure PC and (b) 1 M $LiPF_6$/PC : DEC (4 : 1, v/v) at a low rate of 0.5 mA/cm².
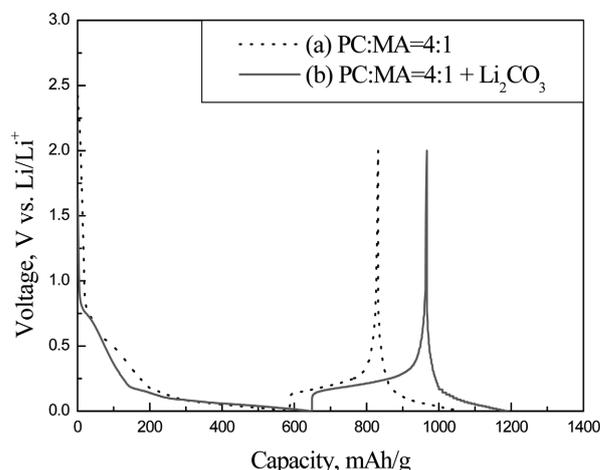
Figure 2. Voltage-capacity profiles of the KMFC electrode in (a) 1 M $LiPF_6$/PC : MA (4 : 1, v/v) and (b) 1 M $LiPF_6$/PC : MA (4 : 1, v/v) + Li_2CO_3 at a low rate of 0.5 mA/cm².

undergo intercalation and exfoliation occurred by solvent decomposition with gas evolution. The initial charge curve for an KMFC electrode in 1 M $LiPF_6$/PC : DEC (4 : 1, v/v) was similar in behavior to that when PC was used as a single solvent.

Figure 2 shows voltage-capacity profiles of an KMFC electrode in 1 M $LiPF_6$/PC : MA (4 : 1, v/v) and 1 M $LiPF_6$/PC : MA (4 : 1, v/v) + Li_2CO_3 at a low rate of 0.5 mA/cm². The voltage plateau by PC decomposition at 0.8 V (*vs.* Li/Li^+) was effectively suppressed when an electrolyte containing the MA electrolyte was used as a co-solvent. This provides clear evidence that the MA electrolyte suppresses PC decomposition on the KMFC electrode surface. This suggests that a stable passivation film is formed in an electrolyte containing PC by the MA electrolyte of the decomposition products on the KMFC electrode. Accordingly, a stable passivating layer is formed during the initial intercalation in a half-cell using the MA electrolyte as a co-solvent of the PC electrolyte, which covers the KMFC
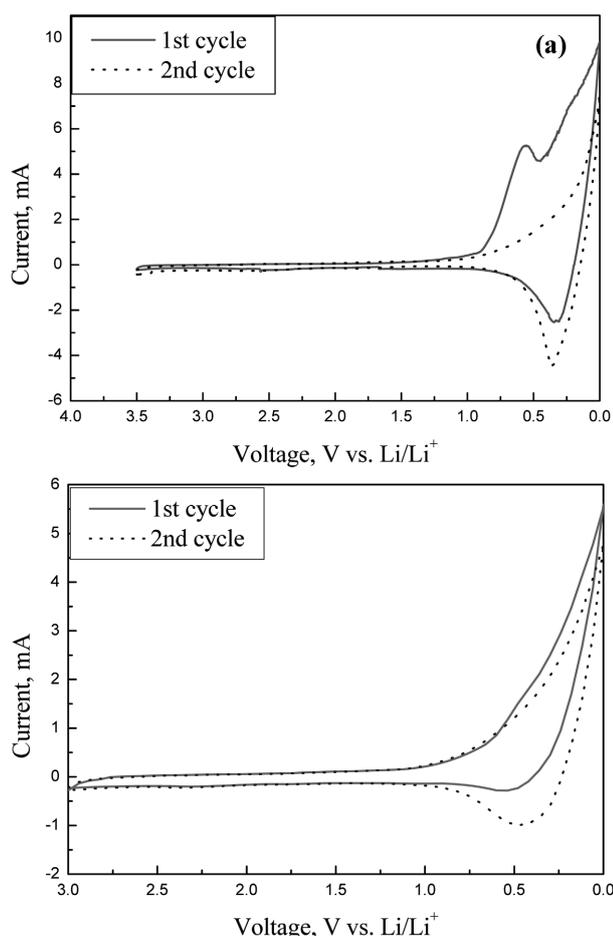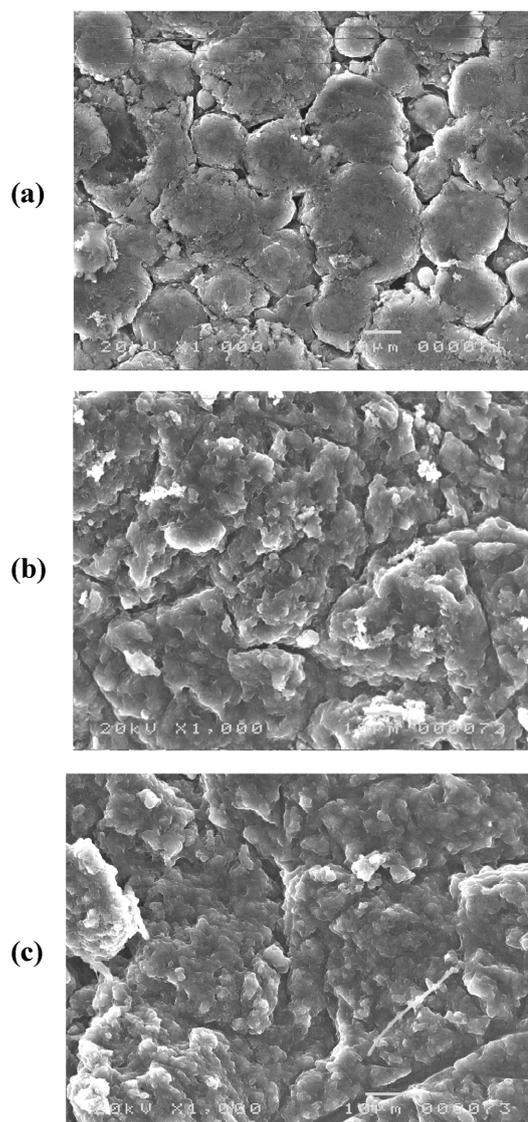
Figure 3. Cyclic voltammograms of the KMFC electrode in (a) 1 M LiPF$_6$/PC : MA (4 : 1, v/v) and (b) 1 M LiPF$_6$/PC : MA (4 : 1, v/v) + Li$_2$CO$_3$.

Figure 4. SEM images of the KMFC electrode surface in (a) bare, (b) 1 M LiPF$_6$/pure PC, and (c) 1 M LiPF$_6$/PC : DEC (4 : 1, v/v).

electrode. The film acts as a screen that filters out solvated molecules of the PC electrolyte allowing only the migration of Li$^+$ into the KMFC layers. Consequently, the passivation film formed by MA decomposition prevents the co-inter-calation of the PC electrolyte and exfoliation of the KMFC electrode. The decomposition of the PC electrolyte on the KMFC electrode in an electrolyte with Li$_2$CO$_3$ is suppressed to a greater extent than that of the electrolyte without Li$_2$CO$_3$. These results can be attributed to the passivation film formed by adding Li$_2$CO$_3$ in the electrolyte having improved properties.

The suppression of solvent decomposition by the addition of MA and Li$_2$CO$_3$ can be clearly seen in cyclic voltammo-grams, as shown in Figure 3. The latter figure is a compari-son of cyclic voltammograms of a KMFC electrode in 1 M LiPF$_6$/PC : MA (4 : 1, v/v) and 1 M LiPF$_6$/PC : MA (4 : 1, v/v) containing Li$_2$CO$_3$.

In the case of 1 M LiPF$_6$/PC : MA (4 : 1, v/v), the reduc-tion peaks caused by PC decomposition have nearly disap-peared. It is clear that PC decomposition at 0.8 V (*vs.* Li/Li$^+$) was suppressed when MA was used as a co-solvent. It would appear that the MA decomposition products were deposited on the KMFC electrode surface before reaching the voltage

for PC decomposition, and, as a result, the electrolyte using MA as a co-solvent did not cause exfoliation. This indicates that the PC solvent did not melt the passivation film formed by the decomposition of MA. Therefore, the passivation film formed by the decomposition of MA inhibited PC decom-position and co-intercalation on the KMFC electrode. No peaks corresponding to solvent decomposition appeared in a second scan, which is consistent with the SEM images. The suppression of solvent decomposition by the added Li$_2$CO$_3$ can be clearly seen in the cyclic voltammograms shown in Figure 3(b). In the case of the electrolyte added Li$_2$CO$_3$, reduction peaks caused by the decomposition of PC are strongly suppressed and the cathodic peak of MA at approxi-mately 0.6 V (*vs.* Li/Li$^+$) has disappeared. This suggests that the passivation film formed by electrolyte added Li$_2$CO$_3$ was superior to that in which MA was used as a co-solvent.

To confirm the above results, the surface morphologies of the KMFC electrode were observed by scanning electron

microscopy (SEM). The original KMFC electrode surface was initially measured in order to compare it with the initial intercalated electrode surface. The original KMFC electrode surface, in which carbon beads are distributed, is shown in Figure 4(a). The diameter of the KMFC electrode was not regular for particle sizes of less than 20 μm. After the intercalation of Li^+ into the KMFC electrode in the 1 M $LiPF_6$/pure PC electrolyte, the deposited KMFC electrode surface was investigated and this result is shown in Figure 4(b). The surface of the intercalated KMFC electrode has a clearly different surface morphology from the original electrode surface. The morphology of the KMFC electrode after the 1st intercalation in the PC electrolyte was changed, compared to the original KMFC electrode. These morphological changes can be attributed to exfoliation of the KMFC electrode by continuous PC decomposition. Therefore, KMFC electrode rapidly undergoes exfoliation when it is charged in 1 M $LiPF_6$/pure PC. As can be seen in Figure 4(c), the KMFC electrode was also destroyed in 1 M $LiPF_6$/ PC : DEC (4 : 1, v/v).

Figure 5(a) and 5(b) shows the lithiated KMFC electrode in 1 M $LiPF_6$/PC : MA (4 : 1, v/v) and 1 M $LiPF_6$/PC : MA (4 : 1, v/v) + Li_2CO_3. As shown Figure 5(a) and 5(b), both the morphology of the KMFC electrode in 1 M $LiPF_6$/PC : MA (4 : 1, v/v) and 1 M $LiPF_6$/PC : MA (4 : 1, v/v) + Li_2CO_3 did not undergo exfoliation, as in 1 M $LiPF_6$/pure PC. These results indicate that the stable passivation film formed by MA as a co-solvent of the PC electrolyte prevented the co-intercalation of solvent into the graphene layers which resulted in exfoliation of the KMFC electrode. The more compact passivation film formed by the electrolyte added
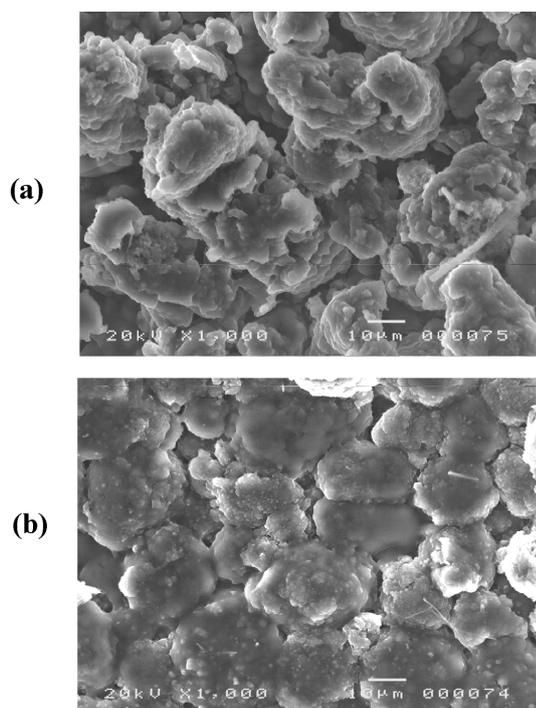
Figure 5. SEM images of the KMFC electrode surface in (a) 1 M $LiPF_6$/PC : MA (4 : 1, v/v), and (b) 1 M $LiPF_6$/PC : MA (4 : 1, v/v) + Li_2CO_3.
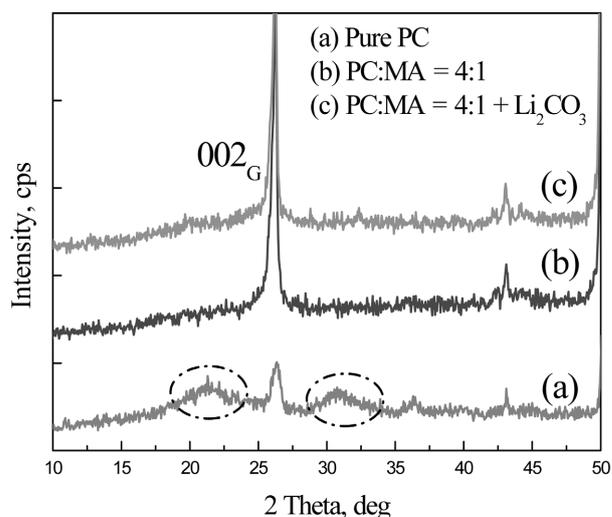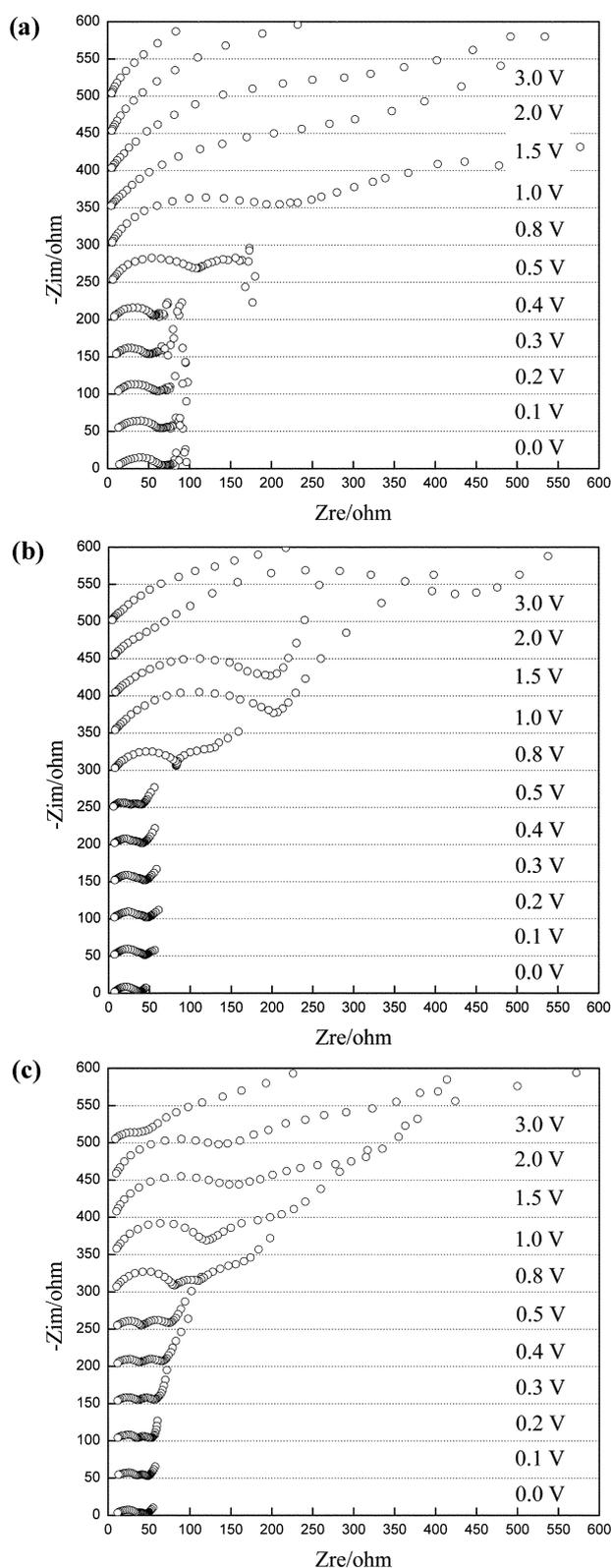
Figure 6. XRD patterns of the KMFC electrode after intercalation in (a) 1 M $LiPF_6$/pure PC, (b) 1 M $LiPF_6$/PC : MA (4 : 1, v/v), and (c) 1 M $LiPF_6$/PC : MA (4 : 1, v/v) + Li_2CO_3.

Li_2CO_3 as an additive has excellent properties and results in a fine deposit of encapsulated KMFC beads. The film was dense and no dissolution of the PC electrolyte was evident. These results were also consistent with voltage-capacity profiles and XRD data.

To investigate the structure of the SEI formed by solvent decomposition, an XRD analysis was performed after the 1st charge in these electrolytes. These results are shown in Figure 6. Several (002) peaks corresponding to graphite carbon were detected at about 26°. However, the XRD pattern of the KMFC electrode in the pure PC electrolyte was clearly different from that for the electrolyte to which MA and Li_2CO_3 were added. In the pure PC electrolyte, the broad region is indicative of an amorphous phase and is believed to be due to structural changes by PC decomposition. As a result, we conclude that MA and Li_2CO_3, when added to the electrolyte, prevented co-intercalation by PC decomposition, thus preventing the destruction of the KMFC electrode structure.

Figure 7 shows impedance spectra measured at various potentials during the initial charge process. This figure is a comparison of the impedance spectra of a KMFC electrode in 1 M $LiPF_6$/pure PC, 1 M $LiPF_6$/PC : MA (4 : 1, v/v) and 1 M $LiPF_6$/PC : MA (4 : 1, v/v) containing Li_2CO_3. The measured potential is 3.0, 2.0, 1.5, 1.0, 0.8, 0.5, 0.4, 0.3, 0.2, 0.1 and 0.0 V (*vs*. Li/Li^+) in the frequency range from 64 kHz to 0.01 Hz. The interpretation of the impedance spectra is based on a simple equivalent circuit model proposed by Takami *et al*.[19] The diagrams (Figure 7) show two semicircles on a complex plane. The semicircle in the high frequency region corresponds to the SEI film and those in a low frequency are derived from charge transfer between the electrolyte and the electrode interface. Film resistance was uniform in the high frequency range for the case of the SEI film formed by 1 M $LiPF_6$/PC : MA (4 : 1, v/v) and 1 M $LiPF_6$/PC : MA (4 : 1, v/v) + Li_2CO_3. The film resistance, as

Figure 7. Impedance spectra of the KMFC electrode in (a) 1 M LiPF₆/pure PC, (b) 1 M LiPF₆/PC : MA (4 : 1, v/v), and (c) 1 M LiPF₆/PC : MA (4 : 1, v/v) + Li₂CO₃.

the result of 1 M LiPF₆/Pure PC was, however, changed in the high frequency region during the film formation process. Continuous PC decomposition did not allow the formation

of compact surface films. Based on this result, the SEI film on the KMFC electrode in 1 M LiPF₆/PC : MA (4 : 1, v/v) and 1 M LiPF₆/PC : MA (4 : 1, v/v) containing Li₂CO₃ appears to be very stable, compared to an electrolyte containing only PC.

Conclusions

Methyl acetate (MA) and lithium carbonate (Li₂CO₃) were added to a propylene carbonate (PC) containing electrolyte in order to prevent the co-intercalation of PC. It was revealed by voltage-capacity profiles, SEM images, and XRD data that the addition of MA and Li₂CO₃ suppressed the exfoliation of KMFC electrode caused by a continuous PC decomposition. The a.c. impedance spectra showed that the passivation film in the MA and Li₂CO₃ containing PC electrolyte had lower resistance than that formed in the PC only electrolyte. In comparison with the porous passivation film in a pure PC electrolyte, the electrolyte containing MA as a co-solvent and Li₂CO₃ as an additive exhibited two advantages of suppressing the decomposition of PC and forming a stable SEI film with low resistance.

References

1. Arakawa, M.; Yamaki, J.-I. *J. Power Sources* **1995**, *54*, 250.
2. Shu, Z. X.; McMillan, R. S.; Murray, J. J. *J. Electrochem. Soc.* **1995**, *140*, 2873.
3. Dey, A. N.; Sullivan, B. P. *J. Electrochem. Soc.* **1970**, *117*, 222.
4. Fong, R.; Van Sacken, U.; Dahn, J. R. *J. Electrochem. Soc.* **1990**, *137*, 2009.
5. Aurbach, D.; Ein-Eli, Y.; Chusid, O. Y.; Carmeli, Y.; Babai, M.; Yamin, H. *J. Electrochem. Soc.* **1994**, *141*, 603.
6. Aurbach, D.; Chusid, O. Y.; Carmeli, Y.; Babai, M.; Ein-Eli, Y. *J. Power Sources* **1993**, *43*, 47.
7. Aurbach, D.; Ein-Eli, Y.; Markovsky, B.; Carmeli, Y.; Yamin, H.; Luski, S. *Electrochim. Acta* **1994**, *39*, 2559.
8. Dahn, J. R.; Fong, R.; Spoon, M. J. *Phy. Rev. B* **1990**, *42*, 6424.
9. Abe, T.; Kawabata, N.; Mizutani, Y.; Inaba, M.; Ogumi, Z. *J. Electrochem. Soc.* **2003**, *150*, A257.
10. Shu, Z. X.; McMillan, R. S.; Murray, J. J. *J. Electrochem. Soc.* **1993**, *140*, 922.
11. Naji, A.; Ghanbaja, J.; Willmann, P.; Billaud, D. *Electrochim. Acta* **2000**, *45*, 1893.
12. Zhang, X.; Kostecki, R.; Richard Son, T. J.; Pugh, J. K.; Ross, Jr, P. N. *J. Electrochem. Soc.* **2001**, *148*, A 13141.
13. Chung, G. C.; Kim, H. J.; Yu, S. I.; Jun, S. H.; Choi, J. W.; Kim, M. H. *J. Electrochem. Soc.* **2000**, *147*, 4391.
14. Wang, C.; Appleby, A. J.; Little, F. E. *J. Electroanal. Chem.* **2002**, *519*, 9.
15. Billaud, D.; Naji, A.; Willmann, P. *J. Chem. Soc., Chem. Commun.* **1995**, 1867.
16. Ding, M. S.; Jow, T. R. *J. Electrochem. Soc.* **2003**, *150*, A620.
17. Pan, Q.; Guo, K.; Wang, L.; Fang, S. *J. Electrochem. Soc.* **2002**, *149*, A1218.
18. Zhang, S. S.; Xu, K.; Allen, J. L.; Jow, T. R. *J. Power Sources* **2002**, *110*, 216.
19. Takami, N.; Satoch, A.; Hara, M.; Ohsaki, T. *J. Electrochem. Soc.* **1995**, *142*, 371.